Experimental Verification of the Relativistic Doppler Effect

HIRSCH I. MANDELBERG* AND LOUIS WITTEN
RIAS, Baltimore, Maryland

(Received August 9, 1961)

An experiment has been performed to measure the quadratic Doppler shift, $\sim(1-v^2/c^2)^{-\frac{1}{2}}$, predicted by the special theory of relativity. A moving beam of radiating hydrogen atoms with velocities ranging up to 2.8×10^8 cm/sec has been viewed from the incoming and outgoing directions simultaneously. Averaging wavelength measurements of a particular spectral line for the two observations gives a measurement of the quadratic shift. The number $(\frac{1}{2})$ in the theoretically predicted exponent can be compared to the experimental results. The latter gives the value of this exponent to be 0.498 ± 0.025. The predominant factor leading to the experimental uncertainty is the width of the spectral lines involved in the measurement.

I. INTRODUCTION

COMPARATIVELY few nonnull experiments of interest with regard to the special theory of relativity have been made. The successful design of high-energy machines which accelerate particles over a range of velocities from zero to nearly the velocity of light is a striking confirmation of a nonnull prediction of the theory, that involving the mass variation. A recent analysis[1] has shown that the design and operation of the machines are such that they would work even if there were a discrepancy of several percent between experiment and theory. Recent careful direct measurement[2,3] of the mass-variation law for 385- and 660-Mev protons have given agreement with theory with an accuracy of 0.1 or 0.2%. The agreement between the experimental measurements and the theory of the fine structure of hydrogen shows that the relativistic mass variation law which is assumed in the theoretical analysis is correct with an accuracy of 0.05%.[1]

Another nonnull result of the theory which can be measured is the frequency or Doppler shift of spectral lines and its dependence on the square of the velocity (on $\beta^2\equiv v^2/c^2$) together with the associated time-dilation prediction. A series of measurements of the lifetime of mu mesons moving over a range of velocities well into the relativistic region ($v/c\sim1$), when compared with the rest-frame lifetime of mu mesons, gives agreement with theory within several percent. Atomic beam measurements by Ives and Stilwell[4] and by Otting[5] have been made on the H_α and H_β lines emitted by a beam of fast-moving hydrogen atoms. Their experimental arrangement is substantially the same as that used in the experiment we have performed which will be described in detail below. An analysis[6] of the experiments of Ives and Stilwell and of Otting indicates that although their reported experimental points seem to fit the curve with an accuracy of about 2 to 3%, the experimental uncertainty is more nearly 10–15%. By use of the Mössbauer effect, a measurement of the quadratic term in the Doppler shift has been made under conditions when no first-order shift appears; the velocity involved in the experiment was rather low ($\beta<10^{-6}$).

We wish to report an experiment whose purpose was to measure the quadratic Doppler shift by techniques similar to those introduced by Ives and Stilwell and to establish the limits of accuracy of the method. The experimental result is that the exponent in the quadratic expression for the Doppler shift, $(1-\beta^2)^{-\frac{1}{2}}$, is found to be 0.498 ± 0.025.

II. PRINCIPLE OF EXPERIMENT

In this section we shall outline the ideas behind the experiment. Consider a beam of radiating hydrogen atoms of velocity v observed at an angle θ, near zero. This beam is produced by accelerating hydrogen molecular ions with voltages up to 76 kv or velocities up to 2.8×10^8 cm/sec. These fast molecular ions are then converted to fast excited atoms through collisions with stationary hydrogen molecules.

The wavelength of the light emitted from an oncoming atom of velocity v viewed at a small angle θ to the beam direction by an observer stationary in the laboratory reference frame is given by

$$\lambda_B=\lambda_0\frac{1-\beta\cos\theta}{(1-\beta^2)^{\frac{1}{2}}}\approx\lambda_0(1-\beta\cos\theta+\tfrac{1}{2}\beta^2), \qquad (1)$$

where θ is measured in the laboratory frame and λ_0 is the wavelength observed in a reference frame at rest with respect to the radiating atom. The $\beta\cos\theta$ term in the numerator is the first-order Doppler shift; the subscript B indicates a Doppler shift to the blue. The denominator contains the quadratic shift; the approximate expression is valid in this experiment because of the low velocity ($\beta<0.01$) and the experimental uncertainty. Similarly, the wavelength of the light emitted

---

* Present address: Physical Sciences Division, 7338 Baltimore Blvd., College Park, Maryland.

[1] P. S. Farago and L. Janossy, Nuovo cimento **5**, 1411 (1957).
[2] D. J. Grove and I. C. Fox, Phys. Rev. **90**, 378 (1953).
[3] V. P. Zrelov, A. A. Tiapkin, and P. S. Farago, J. Exptl. Theoret. Phys. (U.S.S.R.) **34**, 384 (1958).
[4] H. E. Ives and G. R. Stilwell, J. Opt. Soc. Am. **28**, 215 (1938); **31**, 369 (1941).
[5] G. Otting, Physik, Z. **40**, 681 (1939).
[6] H. I. Mandelberg, Ph.D. dissertation The Johns Hopkins University, 1960 (unpublished). RIAS Technical Report 60-20 is substantially the same as the dissertation and is available by writing to the RIAS librarian. This report contains many details of the experiment which are not reported here.

in the backward direction, i.e., as seen by a laboratory fixed observer looking at a receding atom, is given by

$$\lambda_R=\lambda_0\frac{1+\beta\cos\theta}{(1-\beta^2)^{\frac{1}{2}}}\approx\lambda_0(1+\beta\cos\theta+\tfrac{1}{2}\beta^2), \quad (2)$$

the subscript R indicating a red Doppler shift. The average of these two wavelengths,

$$\lambda_Q\equiv\tfrac{1}{2}(\lambda_B+\lambda_R)=\lambda_0(1+\tfrac{1}{2}\beta^2), \quad (3)$$

equals the wavelength which would be observed at right angles to the beam, corresponding to $\theta=\pi/2$ in Eqs. (1) and (2). There are many reasons why a perpendicular observation of the beam is not feasible, the foremost among these being the difficulty of achieving the extremely accurate alignment necessary to reduce the first-order Doppler shift to a size sufficiently smaller than the second-order effect to make accurate measurement of the second-order effect possible.

The experiment consisted in measuring λ_R and λ_B, the wavelengths observed with and opposite to the beam, and taking the average to determine λ_Q and hence $\lambda_0\beta^2/2$. By a subtraction,

$$2\lambda_D\equiv\lambda_R-\lambda_B=2\lambda_0\beta\cos\theta, \quad (4)$$

β was determined by measuring λ_R, λ_B, λ_0, and θ. The velocity was thus obtained by direct measurement without assuming a precise knowledge of the accelerating voltage and without making assumptions regarding the collision mechanism which produced the atom. To give an idea of the magnitudes of the parameters involved, a typical run was made with an accelerating voltage of 63.70 kv which produced a beam of excited atoms whose measured velocity corresponded to $\beta=0.008176$. For a wavelength $\lambda_0=6562.793$, we measured $2\lambda_D=107.317$ A and $\delta\lambda\equiv\frac{1}{2}\lambda_0\beta^2=0.219$ A.

III. DESCRIPTION OF EXPERIMENT AND APPARATUS

The apparatus for this experiment can be divided into two major categories, that for the production and that for the observation of the radiating atomic beam. The apparatus for the production of the collimated beam consists of an ion source and associated electrical

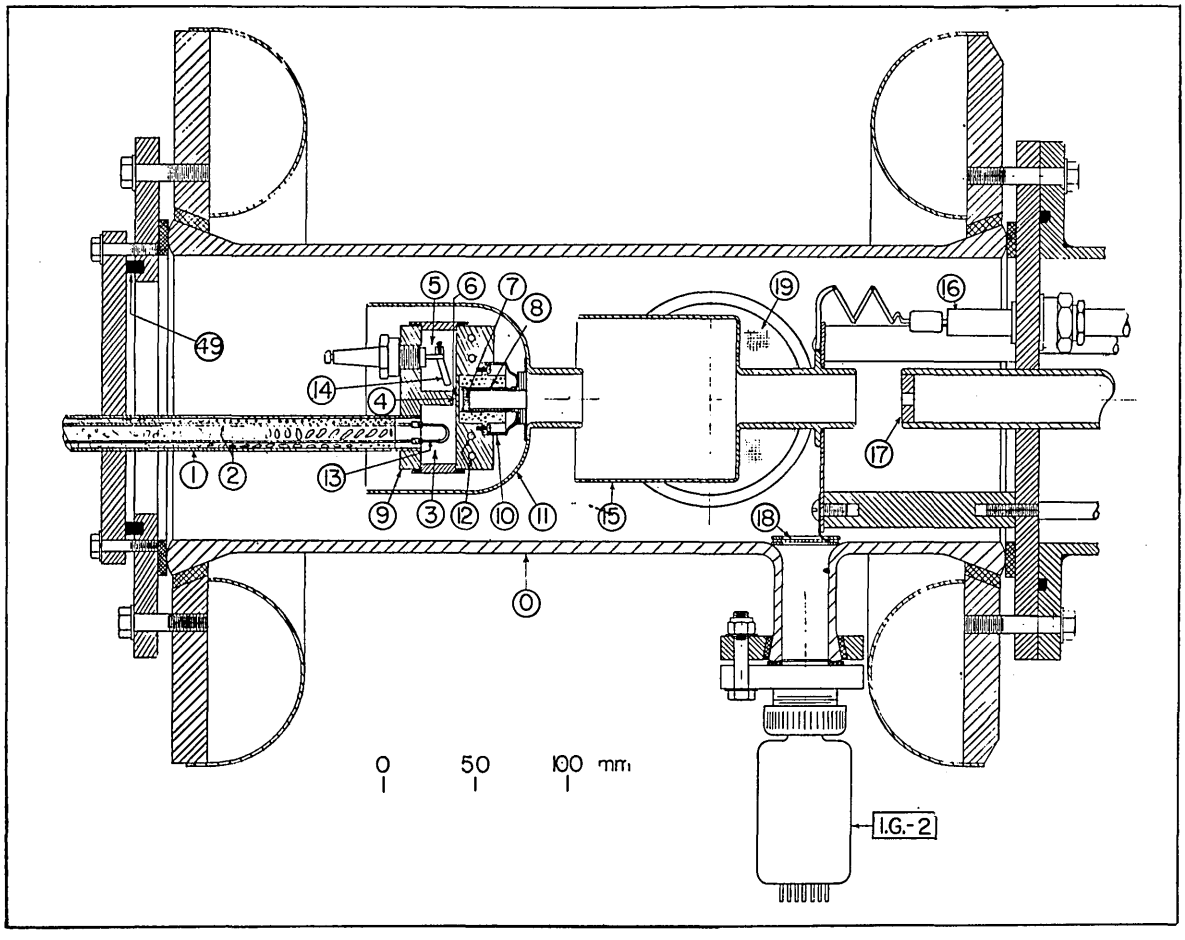

FIG. 1. Ion source and acceleration chamber: (3) oxide coated filament, (4) capillary, (6) beam exit aperture, (7) probe, (9) arc block, (11) probe corona shield, (14) anode, (15) accelerating electrode. For all other components, see reference 6.

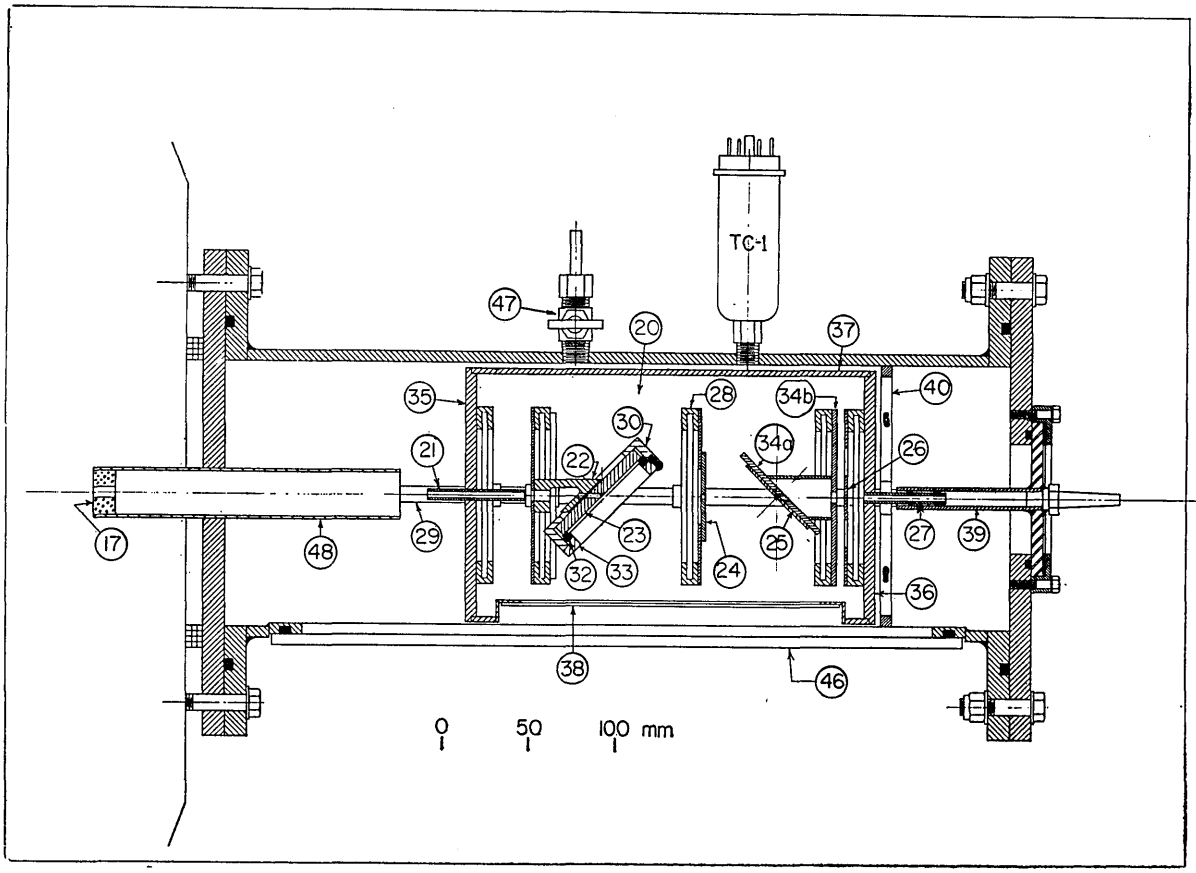

FIG. 2. Observation chamber: (*20*) inner observation chamber, (*21*) beam entrance tube, (*22*) mask, (*23*) "Red" mirror, (*24*) mask, (*25*) "Blue" mirror, (*26*) stopping plate, (*27*) hydrogen inlet tube, (*38*) inner chamber window, (*46*) main window. For other components, see reference 6.

circuitry which produced the ion beam (i.e., a power supply, electrostatic focusing system and circuitry which accelerate and collimate the beam from the low-velocity ions emitted by the source) and an observation chamber where the high-velocity ions are converted into high-velocity excited atoms which emit H_α radiation. The excitation process is a collision between a fast molecular ion and a molecule stationary in the observation chamber and can be described by the processes (5) and (6):

$$\text{fast } (H_2^+) + \text{stationary } H_2 \rightarrow \text{fast } H^* + \text{other products}, \quad (5)$$

$$\text{fast } (H_3^+) + \text{stationary } H_2 \rightarrow \text{fast } H^* + \text{other products}. \quad (6)$$

The fast excited atom has almost the same velocity as the incident molecular ion. Since the excitation mechanism is a collision, the pressure in the observation chamber should be high enough to get as many single collisions as possible but not high enough to get a substantial number of multiple collisions.

The observation system consists of mirrors and lenses which view the beam symmetrically from the beam and antibeam directions, combines the light from these two directions, and sends it through a Fabry-Perot etalon crossed with a grating spectrograph which provides the requisite spectral dispersion.

The vacuum system in which the atomic beam was produced and observed is shown in Fig. 1 (the acceleration chamber), Fig. 2 (the observation chamber), and Fig. 3 (the electrical connections). The capillary-arc

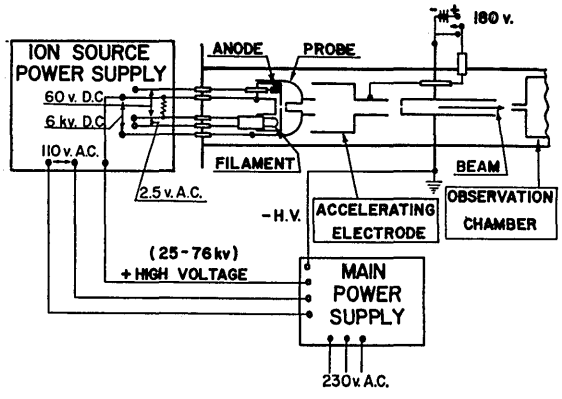

FIG. 3. Ion beam circuitry.

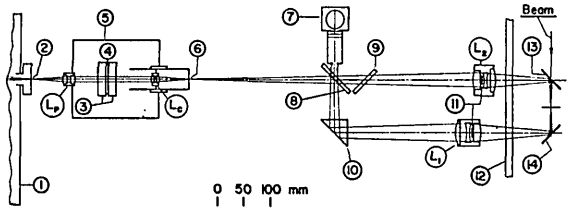

FIG. 4. Optical system: (*1*) 1.5-m Wadsworth spectrograph, (*2*) 200-micron slit, (*3*) interferometer plates, (*4*) 1 mm spacer, (*5*) temperature controlled interferometer housing, (*6*) 400-μ slit, (*7*) monitor photomultiplier, (*8*) half reflecting mirror, (*9*) axis correction plate, (*10*) prism, (*11*) central masks, (*12*) main vacuum system window, (*13*) "red" mirror, (*14*) "blue" mirror, (L_1) 152 mm focal length $f/3.5$ lens, (L_2) 135 mm focal length $f/3.5$ lens, (L_c) 60 mm focal length $f/5.6$ lens, (L_p) 90 mm focal length $f/6.8$ lens.

type of ion source (No. *1–14* of Fig. 1) was borrowed from Allison. He has described elsewhere[7] the details of construction and operation of this ion source. After being produced by the ion source, the beam is accelerated to the full voltage of the high-voltage power supply by electrode *15*. A typical ion-beam current is 100 μa. The beam passes into the observation chamber (Fig. 2). It then passes through tube *21* into the inner observation chamber, whose only opening to the outer chamber is through this tube. The ion beam then passes through mask *22* which protects the mirror M_R, *23*, from the direct impact of the beam. The beam goes through an 0.093-in. diameter hole in M_R, then through mask *24*, and through an 0.093-in. diameter hole in M_B, *25*. Hydrogen is admitted into the inner observation chamber through the tube *27*. The pressure inside this chamber is thereby maintained at about 400 μ of Hg. Collisions of the fast hydrogen ions with stationary molecules excite the ion beam to a bright glow. Doppler-shifted lines are observed corresponding to hydrogen atoms produced from H_2^+ and H_3^+, respectively, and moving with velocities approximately equal to $(2eV/2m_0)^{\frac{1}{2}}$ and $(2eV/3m_0)^{\frac{1}{2}}$, where V is the accelerating potential and m_0 is the mass of a proton. Fast pumps maintain the acceleration chamber pressure at 2×10^{-4} mm Hg.

The beam of radiating atoms is then observed by means of the optical system shown in Fig. 4. Lenses L_1 and L_2 focus the light from each direction from a point midway between M_R and M_B, through a prism P and half-reflecting mirror $M_{\frac{1}{2}}$ onto a 400 μ slit in front of the Fabry-Perot etalon. The axis-correcting plate corrects for the lateral displacement of the optic axis of the lens L_2 caused by refraction through the $\frac{1}{4}$-in. thickness of $M_{\frac{1}{2}}$. The light is collimated by lens L_c and passed through the etalon which has a 1-mm spacer and whose plates have a silver coating with a half-wave coating at H_α of SiO. This gives each plate a reflectance at H_α of 70%; and the interferometer, an interferometer efficiency $[T/(T+A)]^2$ of 75%; T being the transmittance and A the absorptance of each reflecting film.

[7] S. K. Allison, Rev. Sci. Instr. 19, 291 (1948).

The interferometer fringe system is focused, together with the image of the beam, on the 200-μ slit of a 1.5-m Wadsworth spectrograph. This system provides a linear dispersion on the photographic plate which is approximately ten times that of the 1.5-m Littrow mount spectrograph which had been used by Ives and Stilwell. The optical system is such as to magnify the 2-mm beam diameter to cover a 10-mm height on the spectrograph slit which is sufficient to give five complete interference fringes for measurement.

The main power supply, which generates the high electrostatic potential with which the beam is accelerated, was designed and built on special order by the NJE Corporation, Kenilworth, New Jersey (their model No. 46H59). The output voltage can be varied continuously from 10 to 80 kv and is stable to $\pm0.007\%$ over a 24-hr period with a negligibly small hum and noise level and with an output current up to 10 ma. A tap on the main voltage divider is provided that produces a small voltage (3 v max) which can be used for monitoring the potential. This voltage was monitored during a run by a John Fluke differential dc voltmeter having a accuracy of 0.002%. The monitoring tap and differential dc voltmeter permitted the high-voltage output to be set before the run to within 0.1% of the desired value and also permitted checking the stability of the power supply which remained within the specified tolerance of $\pm0.007\%$ over a 24-hr period.

IV. APPARATUS DESIGN CONSIDERATIONS

Some of the special points of interest in the design of the experiment are briefly outlined.

A. Velocity or Voltage Stability

A variation of the velocity of the atoms in the beam would produce a variation in the first-order Doppler shift λ_D, which would shift the spectral line considerably. Obviously $\lambda_D\sim\beta$ or $\lambda_D\sim V^{\frac{1}{2}}$, where V is the accelerating potential. Hence

$$\delta\lambda_D/\lambda_D=\tfrac{1}{2}\delta V/V. \tag{7}$$

For the power supply used $\delta V/V=7\times10^{-5}$; hence $|\delta\lambda|<0.002$ A for $\lambda_D=60$ A (the maximum attained in the experiment). Therefore, 0.002 A was arbitrarily set as the limit within which other errors should be kept.

B. Alignment Errors

As can be seen from Fig. 4, the observation angle θ varies from almost zero to the angle subtended by the outermost portions of the focusing lenses L_1 and L_2. Because of the cylindrical symmetry around the beam axis, all the light emitted by the beam in the angular range of interest is intercepted by the optical system. To determine the precision required in the alignment of the optics, it is sufficient, because of this symmetry about the beam, to consider the effect of a misalignment of a zero-aperture optical system, which ideally is

aligned along the beam. For this model, $\lambda_D \equiv \lambda_D(\theta=0) = \lambda_0\beta$. If now the system is misaligned by a small angle θ, $\lambda_D = \lambda_0\beta\cos\theta \approx \lambda_D(1-\theta^2/2)$, and the error caused by the misalignment is $\frac{1}{2}(\lambda_D)\theta^2$. If this error is to be kept below 0.001 A, the resultant condition on the alignment error is that $\theta < 0.005$ rad.

C. Collimation Effects

The atomic beam is not a perfectly parallel beam but has some angular divergence. However, because of the cylindrical symmetry of the beam and viewing mirrors, M_R and M_B, and because of the symmetry of the optical system about the common focal point of the lenses, L_1 and L_2, the only effect of the divergence is to increase the effective viewing angle or aperture of the optical system. No asymmetry of aperture between the beam and antibeam observations is introduced. Measurements of the beam divergence were made with a cathetometer as the beam traveled down the observation chamber. The measured divergence was about 0.25 deg which agrees with estimates that can be made from experiments using counting techniques.[8]

D. Stark Effect

Another factor to consider is the shift in the wavelength of the emitted line caused by the Stark effect arising from the fact that the radiating atoms are in an electric field caused by the ion beam. The fields encountered can be estimated from a knowledge of the beam current, radius, and velocity and turn out to be of the order of 10 v/cm. The shift in the wavelength of the H_α lines due to quadratic Stark effect is much less than the 0.002 A error tolerance and can be ignored.

E. Aperture Effects

Most of the effort in the design of the optical system used in the experiment went into ensuring that aperture effects would introduce no significant errors. The important point here is that the major contribution to the linewidth is that due to the variation in λ_B and λ_R caused by the variation in θ due to the finite size of the aperture. The variation in observed wavelength goes as $\cos\theta$, which is an even function of θ; i.e., a larger aperture will give a broader line, and its width will increase only toward smaller values of λ_R and larger values of λ_B, thereby causing a shift in the apparent center of the lines. For this reason the angular apertures used in viewing the light from the beam and antibeam directions must be closely matched. If this is not done, the asymmetry of first-order Doppler shifts from aperture asymmetries could cause large errors in the measurement of the quadratic effect. Now let us consider the required symmetry. Since $\lambda_{D(\text{minimum})} = \lambda_0\beta \times\cos\theta_{\max}$, $d(\lambda_{D\ \min}) \approx \lambda_0\beta\theta_{\max}d\theta_{\max}$ for small $\theta_{\max}$ (maximum viewing angle). An error of 0.004 A is allowable here for the shift of wavelength at the edge of the line; this corresponds to a shift of the center of 0.002 A.

For the optical system used in this experiment, assuming that the limiting stop of the entire optical system is at the spectrograph collimating mirror, it can be shown[6] that the maximum viewing angle $\theta_{\max}$, for either lens L_1 or L_2 is given by

$$\theta_{\max} = (A/2)(f_p/f_c)m.$$

A is the spectrograph aperture, f_p and f_c are the focal lengths of the interferometer projection and collimation lenses, respectively, and m is the lateral-magnification factor of L_1 or L_2 for projecting an image of the beam on the interferometer slit. Therefore, even though L_1 and L_2 must have different focal lengths because of the mechanical arrangement, it is only necessary that their respective lateral-magnification factors be matched. For the tolerances allowed here, it is necessary to choose focal lengths and distances such that the magnification factors of L_1 and L_2 ($m \approx 3$) will be matched to 1%.

Another important point in the design of the optical system is the requirement that every point on the image of the beam upon the spectrograph slit be illuminated by light from the same angular range with respect to the beam axis. Because of the $\cos\theta$ dependence of the Doppler shift, any variation in angular range would cause a variation in wavelength along the spectrograph slit, thereby rendering the interferometer fringes meaningless. An analysis[6] will show that this requirement can be satisfied by the proper choice of the distance between the interferometer collimation and projection lenses, and is critically dependent upon this distance. For this reason the collimation lens was mounted in a movable collar, a light source was set up inside the spectrograph and the collimation lens was adjusted until the effective apertures of the focusing lenses were independent of slit height. The change in the magnification factors of L_1 and L_2 because of this motion is a second-order effect and has no significant effect on the magnification-matching condition.

Masks were inserted in the focusing lenses to eliminate the light originating from the central 5-mm diameter of the internal mirrors because the beam destroyed this portion of the surface of the blue mirror (*25*, Fig. 2) after a short time. This portion of the blue mirror and the identical portion of the red mirror had to be masked off to preserve the angular symmetry. Finally, the depth of field of this optical system, due to the high longitudinal-magnification factor of 20, was less than 1 mm; therefore no variations in $\theta_{\max}$ could arise from a large depth of field.

V. EXPERIMENTAL PROCEDURE

The internal mirrors (M_R and M_B) were aligned within ± 0.002 in. and the external optics were aligned

[8] D. R. Sweetman, Proc. Roy. Soc. (London) **A256**, 416 (1960).

to the smaller of ± 0.003 in. or 0.001 rad. The data runs were taken over a period of 6 months. Immediately prior to each run the alignment of the entire system was checked by using a light source in the spectrograph. Referring to Fig. 4, it is obvious that in this configuration L_1 and L_2 have mutual focal points. Therefore the image of a light source in the focal plane of L_c, i.e., at the collimator slit, will be focused back onto itself, provided the system is in perfect alignment. In checking the alignment, such a light source was provided by imaging a light source inside the spectrograph onto the collimator slit. If the system is misaligned in some fashion, the image as focused back in the collimator focal plane will not be in register with its object and this lack of register can be visually detected. It can be demonstrated, for the optical system in use, that this method can detect an error of 0.001 rad in the central viewing angle. This provides an adequate verification of the alignment of the optical system.

Data runs were taken for operating voltages between 24.50 and 76.00 kv. The voltages were chosen so as to allow ± 0.4 A clearance between the "beam" lines (Doppler-shifted H_α lines) and the lines of the hydrogen molecular spectrum. Some of the resultant "allowed" voltage ranges, where none of the four (red and blue shifted mass 2 and red and blue shifted mass 3) beam lines were within 0.4 A of a molecular line, were rather narrow. This necessitated that the accelerating voltage be known fairly accurately. As has already been remarked, by calibrating the output voltage against the voltage from a low voltage (1–3 v) tap on the power-supply divider chain, it was possible to set the accelerating voltage to $\pm 0.1\%$, by the use of a precision (0.001%) voltmeter.

After checking the optical-system alignment, and stabilizing the beam operation, reference exposures were made with a neon discharge tube. The exposure was then made on Kodak 103aE plates, varying in time from 5 to 25 hr, depending on the light intensity. Another reference exposure was made following the run, after which the system alignment was again checked. During the exposure the interferometer-housing temperature was maintained at a constant value within ± 0.01°C; the housing was sealed against atmospheric pressure changes. The limitation on the exposure time arose from the fact that stray atoms or ions struck the active part of the blue mirror. There was not enough intensity to destroy the mirror surface rapidly, as was the case in the central part of the beam, but these atoms did cause a polymerization of a surface layer of hydrocarbons from the vacuum grease and backstreaming pump oil. Consequently, a carbon layer built up on the mirror which reduced its reflectivity to about 5% in 24 hr of running time. The carbon layer was assumed to be uniform over the very small region at the center of the mirror whose reflected light entered the interferometer; hence the angular distribution of the light was assumed to be unchanged by the layer. In

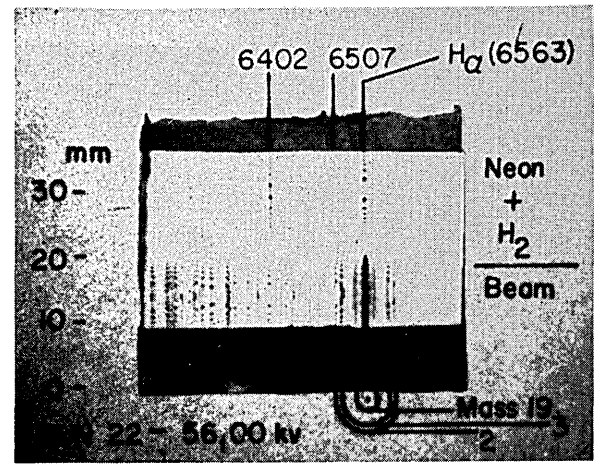

FIG. 5. Sample of photographic plate. Reference is at top, beam spectrum at bottom.

about 75% of the runs a usable density was present on the photographic plates after this exposure time. The blue mirror was then replaced for another run.

A typical plate is shown in Fig. 5. This shows the section around H_α, which is the region of interest. The upper spectrum is the neon reference and the important lines are indicated. The lower spectrum is that of the beam. The broad central line, its width comparable to the interferometer free spectral range, is seen. The Doppler-shifted lines, which were the ones measured, are marked in pairs with the mass of the molecular ion to which their velocity corresponds indicated. Note the presence of mass 2, 3, and 19, the 19 belonging to H_3O^+. Velocities corresponding to proton acceleration were observed very weakly on some plates; these were, however, too weak to measure accurately. The low intensity of these lines can be attributed to two factors; a low percentage of protons in the beam, and a low cross section for electron capture as compared to the cross sections for the molecular collisions. The other sharp lines are molecular hydrogen lines. By direct comparison of two plates taken at different voltages, it was determined that there was no shift in these molecular lines. Since the cross section for the production of fast neutral molecules from the molecular ions of H_2^+ is still one-fourth that for the production of fast atoms,[8] the conclusion to be drawn is that the fast molecules which result from the collision are not in excited states, while many of the atoms are. We have found no other measurements that can verify this point.

VI. MEASUREMENTS AND CALCULATIONS

The plates were measured on the photoelectric setting comparator (of the type described by Dieke, Dimock, and Crosswhite[9]) at the Johns Hopkins University spectroscopy laboratory. It has an accuracy of ± 0.25 μ. The neon reference lines measured were those at

[9] G. H. Dieke, D. Dimock, and H. M. Crosswhite, J. Opt. Soc. Am. 46, 456 (1956).

6678.276, 6598.953, 6532.882, 6506.528, 6402.246, 6382.991, and 6266.495 A. The fringe diameters of these lines were treated by the least-squares method described by Meissner[10] to get the fractional order of interference ϵ of each pattern. The method of exact fractions[10] was then used to find the exact order of interference for each fringe pattern. For the closest match between the calculated order of interference and the measured value of ϵ (averaged over 4 measurements of the fringe pattern for each wavelength: 2 on the pre-exposure reference plate and 2 on the post-exposure reference plate), there was a difference which increased with decreasing wavelength. This can be attributed to a phase-shift dispersion with wavelength caused by the SiO protective layer over the silver. The difference between these two numbers, or the phase correction factor, was plotted for all the data runs which were usable and a phase-correction curve obtained. A phase correction from this average curve was then applied in the calculation of the wavelengths of the beam lines.

The wavelengths of the Doppler-shifted H_α lines were calculated by the method of Crosswhite,[11] which utilizes each fringe diameter to get a wavelength determination. This method weights no individual reading more than any other as contrasted with other calculation methods. Hence, a more reasonable idea of the uncertainty in the wavelength measurement can be derived. The method is based on the following considerations. It can easily be shown from the fundamental interferometer equation that

$$\lambda = (2t - CD^2)/n. \tag{6}$$

The interferometer spacer thickness t and the constant C can be derived from the reference line data, and the order of interference at the fringe center n can be observed from an approximate knowledge of λ, the wavelength at the fringe center. D is the fringe diameter. The approximate value of λ is taken from the calculated value by assuming the relativistic shift to be correct.

TABLE I. Calculation of quadratic Doppler shift from data run 15, 68.75 kv, mass 2.

Measured quantities:

$\lambda_R = 6618.808 \pm 0.0075$ A
$\lambda_B = 6507.253 \pm 0.0041$
$\cos\theta = \cos 0.075$ rad $= 0.9972$

Predicted quadratic Doppler shift:

$2\lambda_D = 2\lambda_0\beta\cos\theta = \lambda_R - \lambda_B = 111.555 \pm 0.012$
$2\lambda_0\beta = 111.868 \pm 0.012$
$\beta_{\text{measured}} = 0.0085229 \pm 0.0000001$
$(\frac{1}{2}\lambda_0\beta^2)_{\text{predicted}} = 0.238 \pm 0.0004$

Measurement of $(\frac{1}{2}\lambda_0\beta^2)$:

$\lambda_Q = \frac{1}{2}(\lambda_B + \lambda_R) = 6563.031 \pm 0.006$
$\lambda_0 = 6562.793$ (Taken from literature)
$(\frac{1}{2}\lambda_0\beta^2)_{\text{measured}} = \lambda_Q - \lambda_0 = 0.238 \pm 0.006$

[10] K. W. Meissner, J. Opt. Soc. Am. **31**, 410 (1941).
[11] H. Crosswhite, The Johns Hopkins University Spectroscopic Report No. 13 (1958) (unpublished).

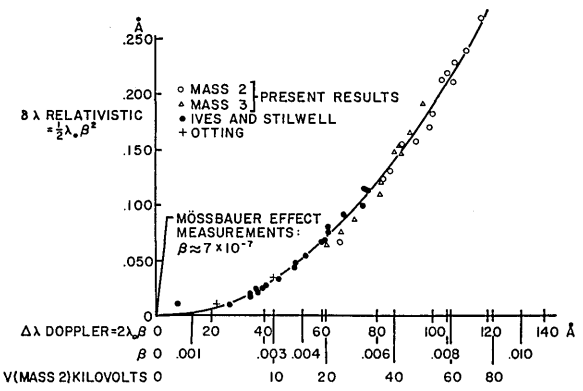

FIG. 6. Results—Relativistic shift as function of first-order Doppler shift and of β. Results of this experiment are shown together with previous results.

This introduces no circularity of argument in the computation, as the assumed value need be accurate to only 1 A. From this, an approximate n can be determined and an unambiguous assignment of the exact order of a given fringe easily made. To this n the phase-correction factor derived from the appropriately prepared curve is added to obtain the true order of interference.

The fringe system for each beam line was measured 4 times to achieve good statistics. Since 4 or 5 fringes were measurable for each line, a total of 16 or 20 wavelengths were calculated. The average of these was determined together with the corresponding uncertainty. The corresponding pair of wavelengths were then treated by Eqs. (3) and (4) to arrive at the measured values of the relativistic shift. The $\cos\theta$ term corresponding to the mean viewing angle of the lenses L_1 and L_2 was taken to be 0.9972. A sample of this calculation is shown in Table I.

The major uncertainty in the beam wavelengths is due to the width of the beam lines themselves. As can be seen from Fig. 5, the width of the lines is about $\frac{1}{3}$ of the free spectral range, which is 2A. The lines are therefore approximately 0.6 A wide, which precluded resolving the doublet nature of H_α. It is possible to locate the center of these to within about 1% of their width, i.e., an uncertainty of about ± 0.006 A is to be expected. This is the approximate value of the uncertainty observed. The uncertainties introduced by systematic errors in alignment, and other causes have been discussed earlier and are small compared to the uncertainty caused by the linewidth. The uncertainty in the spacer thickness t is estimated to give a wavelength uncertainty of ± 0.002 A. The net uncertainty in this measurement is therefore 0.007 A.

The results of this experiment are shown in Fig. 6. The solid line represents the theoretical prediction, the data obtained are indicated as shown. All the plates measured are shown here. None of the deviations is significantly greater than the measured uncertainty of

the individual measurements. The standard deviation of the entire group from the theoretically predicted results is 0.009 A, which is in agreement with the wavelength uncertainties. Since the precision of the measurements is constant in angstroms for all the shifts, the percentage uncertainty is smallest for the higher velocities. It is approximately 3% for the highest velocities measured, up to 16% for the lowest. In the region described approximately by $0.0045<\beta<0.0065$, lie eight consecutive points we have measured, each of which lies below the theoretical line. However, in this region, most of the points measured by Ives and Stilwell lie above the line; taking the experiments together gives a reasonable spread of measured points about the theoretical line in this velocity range.

According to the theory,

$$\delta\lambda_{\text{relativistic}}=K\lambda_0\beta^2; \quad K=\tfrac{1}{2}.$$

A least-squares calculation of the coefficient K was made from the experimental data. The result was $K = 0.498 \pm 0.025$. This implies an over-all precision in this experiment of 5%, the limit on the accuracy being imposed by the width of the beam lines. It is not possible to locate the center of these lines significantly more accurately than has been done here. The other errors, resulting from faulty alignment, aperture effects, voltage variations, etc., are small with respect to the uncertainties arising from the line width; they add only slightly to the experimental uncertainty.

ACKNOWLEDGMENTS

The authors are grateful to Professor S. K. Allison for lending them the ion source and for the valuable advice he gave in the design of the beam acceleration and observation chambers and to Professor G. H. Dieke for his advice and guidance in the design and operation of the optical measurement system. They also wish to thank Professor H. M. Crosswhite, Professor D. E. Kerr, and W. Fastie for helpful discussions and suggestions.

JOURNAL OF THE OPTICAL SOCIETY OF AMERICA VOLUME 52, NUMBER 5 MAY, 1962

Secondary Standards of Ar I and Hg^{198} I in the Near Infrared*

EDSON R. PECK, BAIJ NATH KHANNA, AND N. C. ANDERHOLM
Northwestern University, Evanston, Illinois

(Received September 28, 1961)

A final report is given on wavelength measurements in air of eleven lines of Ar I and three of Hg^{198} I in the near infrared, for use as secondary standards. Measurements of a preliminary character on three other lines are also included. These measurements have been made in the course of several years' time by means of a corner-reflector interferometer of the Michelson type with reversible fringe counter and static fringe interpolator.

COMMISSION 14 of the International Astronomical Union stresses the need of numerous secondary standards of wavelength in the near infrared.[1] It defines class B secondary standards as those known to 0.001 A or better. Concordant measurements by at least two laboratories are required for formal adoption of these standards. The spectra of Ar I and Hg^{198} I have received considerable attention for this purpose because of their ease of excitation, sharpness, and freedom from structure. Photographic measurements of Ar I were made in 1934 by Meggers and Humphreys.[2] A few lines of Ar I were measured in 1953 by Burns and Adams.[3]

Extensive work in both spectra has been reported by Humphreys and Paul.[4,5] They used a Fabry-Perot interferometer whose pattern is scanned by a slit. Littlefield and Rowley[6] have measured the Ar I spectrum relative to the Kr-86 primary standard, by using a reflecting echelon. Rank, Bennett, and Bennett[7] used a Fabry-Perot interferometer with variable air pressure in measuring some infrared lines of Hg^{198}.

The present paper is the report of work which has been done at Northwestern University over a period of several years by means of a corner-reflector interferometer of the Michelson type. This instrument and its manner of use have been described in several papers.[8] Preliminary results were quoted in a paper

* This work has been supported by a research grant from the National Science Foundation. It was begun with the help of three grants from the Research Corporation of New York.

[1] Draft Report of Commission 14 of IAU for meeting of August, 1961.

[2] W. F. Meggers and C. J. Humphreys, J. Research Natl. Bur. Standards 13, 293 (1934).

[3] K. Burns and K. B. Adams, J. Opt. Soc. Am. 43, 1020 (1953).

[4] C. J. Humphreys and E. Paul, Naval Ordnance Laboratory Reports 390, 429, 443 (1958); 464 (1959).

[5] C. J. Humphreys and E. Paul, J. phys. radium 19, 424 (1958).

[6] T. A. Littlefield and W. R. C. Rowley, draft report of Commission 14 for meeting of August, 1961.

[7] D. H. Rank, J. M. Bennett, and H. E. Bennett, J. Opt. Soc. Am. 46, 477 (1956).

[8] E. R. Peck, J. Opt. Soc. Am. 38, 66, 1015 (1948); 45, 795, 931, (1955); E. R. Peck and S. W. Obetz, *ibid.* 43, 505 (1953).